International Journal of Hyperthermia

ISSN: 0265-6736 (Print) 1464-5157 (Online) Journal homepage: informahealthcare.com/journals/ihyt20

# Computer modeling of the combined effects of perfusion, electrical conductivity, and thermal conductivity on tissue heating patterns in radiofrequency tumor ablation

Muneeb Ahmed, Zhengjun Liu, Stanley Humphries & S. Nahum Goldberg

**To cite this article:** Muneeb Ahmed, Zhengjun Liu, Stanley Humphries & S. Nahum Goldberg (2008) Computer modeling of the combined effects of perfusion, electrical conductivity, and thermal conductivity on tissue heating patterns in radiofrequency tumor ablation, International Journal of Hyperthermia, 24:7, 577-588, DOI: 10.1080/02656730802192661

**To link to this article:** https://doi.org/10.1080/02656730802192661

Published online: 09 Jul 2009.

Submit your article to this journal

Article views: 1535

View related articles

Citing articles: 10 View citing articles

Full Terms & Conditions of access and use can be found at
https://informahealthcare.com/action/journalInformation?journalCode=ihyt20

*Int. J. Hyperthermia*, November 2008; 24(7): 577–588

informa
healthcare

# Computer modeling of the combined effects of perfusion, electrical conductivity, and thermal conductivity on tissue heating patterns in radiofrequency tumor ablation

MUNEEB AHMED[1], ZHENGJUN LIU[1], STANLEY HUMPHRIES[2], & S. NAHUM GOLDBERG[1]

[1]*Department of Radiology, Beth Israel Deaconess Medical Center - Harvard Medical School, Boston, Massachusetts and* [2]*Department of Electrical Engineering, University of New Mexico, Albuquerque, New Mexico, USA*

*(Received 6 March 2008; revised 7 May 2008; accepted 9 May 2008)*

**Abstract**

*Purpose.* To use an established computer simulation model of radiofrequency (RF) ablation to characterize the combined effects of varying perfusion, and electrical and thermal conductivity on RF heating.

*Methods*. Two-compartment computer simulation of RF heating using 2-D and 3-D finite element analysis (ETherm) was performed in three phases ($n = 88$ matrices, 144 data points each). In each phase, RF application was systematically modeled on a clinically relevant template of application parameters (i.e., varying tumor and surrounding tissue perfusion: 0–5 kg/m$^3$-s) for internally cooled 3 cm single and 2.5 cm cluster electrodes for tumor diameters ranging from 2–5 cm, and RF application times (6–20 min). In the first phase, outer thermal conductivity was changed to reflect three common clinical scenarios: soft tissue, fat, and ascites (0.5, 0.23, and 0.7 W/m-°C, respectively). In the second phase, electrical conductivity was changed to reflect different tumor electrical conductivities (0.5 and 4.0 S/m, representing soft tissue and adjuvant saline injection, respectively) and background electrical conductivity representing soft tissue, lung, and kidney (0.5, 0.1, and 3.3 S/m, respectively). In the third phase, the best and worst combinations of electrical and thermal conductivity characteristics were modeled in combination. Tissue heating patterns and the time required to heat the entire tumor ±a 5 mm margin to >50°C were assessed.

*Results*. Increasing background tissue thermal conductivity increases the time required to achieve a 50°C isotherm for all tumor sizes and electrode types, but enabled ablation of a given tumor size at higher tissue perfusions. An inner thermal conductivity equivalent to soft tissue (0.5 W/m-°C) surrounded by fat (0.23 W/m-°C) permitted the greatest degree of tumor heating in the shortest time, while soft tissue surrounded by ascites (0.7 W/m-°C) took longer to achieve the 50°C isotherm, and complete ablation could not be achieved at higher inner/outer perfusions (>4 kg/m$^3$-s). For varied electrical conductivities in the setting of varied perfusion, greatest RF heating occurred for inner electrical conductivities simulating injection of saline around the electrode with an outer electrical conductivity of soft tissue, and the least amount of heating occurring while simulating renal cell carcinoma in normal kidney. Characterization of these scenarios demonstrated the role of electrical and thermal conductivity interactions, with the greatest differences in effect seen in the 3–4 cm tumor range, as almost all 2 cm tumors and almost no 5 cm tumors could be treated.

*Conclusion.* Optimal combinations of thermal and electrical conductivity can partially negate the effect of perfusion. For clinically relevant tumor sizes, thermal and electrical conductivity impact which tumors can be successfully ablated even in the setting of almost non-existent perfusion.

**Keywords:** *Radiofrequency, tumor ablation, minimally-invasive therapy, perfusion, mathematical modeling, computer simulation*

## Introduction

Radiofrequency (RF) ablation has been used for the treatment of focal primary and secondary liver malignancies as a minimally invasive, image-guided alternative to standard surgical resection [1–4]. The largest studies and greatest clinical experience

Correspondence: S. Nahum Goldberg, Department of Radiology, Beth Israel Deaconess Medical Center, 330 Brookline Avenue, Boston, MA 02215, USA. Tel: 617-754-2674. Fax: 617-754-2545. E-mail: sgoldber@caregroup.harvard.edu

ISSN 0265–6736 print/ISSN 1464–5157 online © 2008 Informa Healthcare USA, Inc.
DOI: 10.1080/02656730802192661

with RF ablation has been in treating hepatocellular carcinoma, and long-term studies have demonstrated survival outcomes similar to surgical resection or focal tumors <3 cm in diameter [3, 5]. As such, current RF clinical paradigms, including determinations of RF energy deposition and application times, have been developed for liver models, and tailored to hepatic tissue characteristics. However, RF ablation is being increasingly applied for the minimally invasive, image-guided treatment of focal tumors in a wide range of tissue sites, including, kidney [6], lung [7, 8], and bone [9, 10] which have markedly varied tissue characteristics [11, 12].

RF ablation-induced coagulation is dependent upon achieving focal temperatures usually exceeding 50°C for 4–6 min within the designated tissue [13]. The principles of this are characterized by Pennes et al. in the Bioheat equation [14] and further conceptually simplified to describe the basic relationship guiding thermal ablation induced coagulation necrosis as 'coagulation necrosis = energy deposited × local tissue interactions − heat loss' [15]. Prior experimental and clinical studies have demonstrated the importance of intrinsic tissue characteristics, such as tissue perfusion and electrical and thermal conductivity, on RF energy deposition and tissue heating [16–18]. However, given inherent variability of clinical tumor ablation, characterization of the multi-factorial RF energy-tissue interactions is too complex for initial direct clinical interrogation.

More recently, use of computer simulation and modeling of the Bioheat equation has been used to characterize the influence of specific tissue characteristics on RF tissue heating [19–23]. These studies have modulated characteristics individually in both a uniform setting and a two compartment model (with differing inner 'tumor' and outer 'normal background tissue' characteristics), that provides closer simulation to clinical realities. Along these lines, using a two-compartment finite-element model based upon the Bioheat equation, we have confirmed the importance of tumor size, as well as tumor and background perfusion on RF tissue heating patterns and time of ablation [21]. Prior work has also underscored the role of tissue electrical and thermal conductivities on RF heating patterns [20, 24, 25]. Yet, the impact of the interaction between these tissue parameters has not been fully elucidated. The next step in this process, and the purpose of this study, is to use an established two-compartment computer simulation model of RF energy (ETherm) to further characterize the combined effects of varying tumor size, perfusion, and electrical and thermal conductivity on RF heating, particularly for clinically relevant situations and tissue parameters.

## Materials and methods

### *Overview of experimental design*

A two-compartment computer simulation of RF heating using a finite element analysis model (ETherm) was performed (total $n = 88$ matrices, 144 data points each (12 inner perfusion points × 12 outer perfusion points, per map)). Simulated RF application (6–20 min) was systematically modeled for tumor diameters of 2–5 cm on a clinically relevant template of tumor and surrounding tissue perfusion (0–5 kg/m$^3$-s each, in increments of 0.5 kg/m$^3$-s) for internally cooled 3 cm single and 2.5 cm cluster electrodes. In phase I, outer thermal conductivity was changed to reflect three commonly encountered clinical scenarios: soft tissue, fat, and ascites (0.5, 0.23, and 0.7 W/m-°C, respectively). For phase I, 24 matrices were generated (2 electrodes (3 cm single and 2.5 cm cluster) × 3 scenarios × 4 tumor sizes (2–5 cm, 1 cm increments); 144 data point simulations each). In phase II, electrical conductivity was changed to reflect commonly encountered clinical scenarios of normal soft tissue and saline injection within the tumors (0.5 and 4.0 S/m, respectively) for the varied background electrical conductivities of soft tissue, lung, and kidney (0.5, 0.1, and 3.3 S/m, respectively). For phase II, 48 matrices were generated (6 scenarios × 2 electrodes × 4 tumor sizes; 144 data point simulations each). In phase III, the 'best' (i.e., simulating saline injected around the electrode surrounded by soft tissue (electrical inner and outer conductivity of 4.0 and 0.5 S/m, respectively), surrounded by fat (thermal inner and outer conductivity of 0.5 and 0.23 W/m-°C, respectively)) and 'worst' case scenarios (i.e. simulating tumor in kidney (electrical inner and outer conductivity of 0.5 and 3.3 S/m, respectively), surrounded by ascites (thermal inner and outer conductivity of 0.5 and 0.7 W/m-°C, respectively)) combinations of thermal and electrical conductivity were modeled. For phase III, 16 matrices were generated (2 scenarios × 2 electrodes × 4 tumors sizes; 144 data point simulations each). Tissue heating and the time required to heat the entire tumor ±a 5 mm margin to >50°C were assessed, given that these are current commonly used surrogate endpoints for RF ablation [26].

### *Computer simulation model*

All software was provided by Field Precision (Albuquerque, NM) [22, 23]. A two-dimensional finite-element model of coupled RF electric fields and thermal transport was used as a platform for performing computer simulated RF ablation of 3 cm single electrodes, while a three-dimensional model was used for the more complex geometry of

cluster electrodes. Comparative temperature profiles were generated using computer simulation of the electrostatic equations coupled to Pennes' Bioheat equation (ETherm) [27, 28]. Prior versions of this model have been validated as predictive of tissue heating and ablation in *ex vivo* liver [24, 25, 29]. The computer model has been modified with a general control algorithm to permit the generation of matrices of large volumes of data from which we fashioned temperature response surfaces. The model has been previously modified to be biologically relevant, most notably by constructing a temperature limitation control [20]. Specifically, temperature within the model is not allowed to exceed 100°C, the temperature at which boiling limits the ability to apply RF energy (100°C was reached in every simulation) [30]. The model automatically provides the necessary current to achieve up to 100°C heating in the system to a maximum specified current (as would occur clinically, based upon maximum current output of presently available commercial RF generators). When 100°C is achieved at any point in space or time during the simulated RF application, the program automatically reduces the applied voltage to the maximum level at which no tissue is heated beyond this temperature. Thus, our model mimics the biological and physical constraints present during actual RF ablation including experimentally realistic temperature and current limitations. Additionally, for the purposes of this study, simulated perfusion was eliminated for all mesh points that reached a temperature of 50°C to simulate coagulation eliminated microvascular perfusion [31]. Finally, the computer model incorporated varying electrical conductivity according to changes in temperature (with increasing electrical conductivity by 1% for every increase in 1°C), to simulate *in vivo* conditions as demonstrated in prior studies [32].

*Finite-element analysis software*

To simulate a 3 cm single probe of 0.146 cm (17 gauge) in diameter in tumors of different sizes 2 cm, 3 cm, 4 cm, in a cylindrical background tissue of 10 cm in length and 14 cm in diameter, we used the computer program Mesh version 5.0 (Field Precision) to generate conformal triangular meshes. For 2D finite-element calculation for both the electrical and thermal solutions, we used ETherm to performed coupled electro-thermal solutions using the geometry generated by Mesh (Figure 1). To simulate a 2.5 cm cluster electrode in tumors of different sizes in a cylindrical background tissue of 10 cm in length and 14 cm in diameter, we used the computer program MetaMesh (Field Precision) to generate conformal meshes of hexahedrons for the 3D calculations (Figure 1). For 3D finite-element calculation for both the electrical and thermal solutions, we used ETherm3 to performed coupled electro-thermal solutions using the geometry generated by MetaMesh. We used ETherm3 to performed coupled electro-thermal solutions using the geometry generated by MetaMesh.

*Simulated RF application*

RF parameters were selected to best simulate clinical practice using a commonly used electrode system. This included the use of internally cooled electrodes (10°C) of 3 cm tip length single or 2.5 cm tip length cluster, a generator maximum current output of 2000 mA. RF application time varied as specified, ranging from 8–20 min at 500 KHz [2, 33].

*Two compartment model*

In order to assess the wide range of clinically relevant tumor and background characteristics, a previously reported [20] template was used that enabled us to

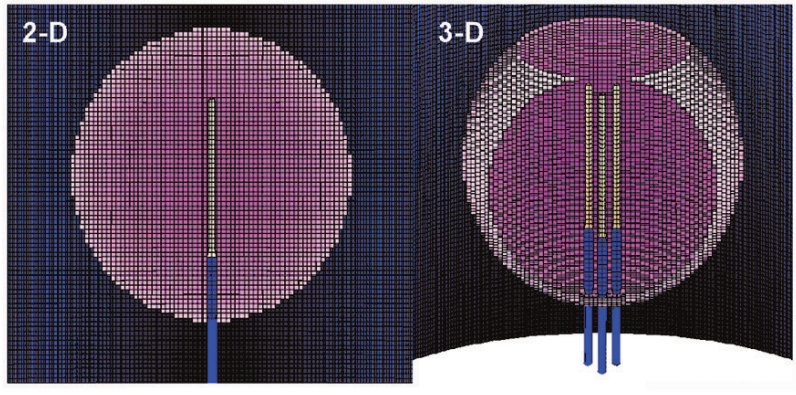


Figure 1. Finite element model meshes. This is an illustrative representation of both the (A) 2D finite element model used for simulating a 3 cm single internally cooled electrode in a 4 cm tumor (as denoted by the purple), and (B) the 3D finite element model used to simulate a 2.5 cm cluster electrode in a 4 cm tumor.

study the effects of a defined parameter space (response contour) consisting of a varied range of tissue perfusion for inner 'tumors' of variable radius, surrounded by uniform tissue parenchyma. A variable sized two-compartment model of 10 cm radius was used. At the innermost region of the cylindrically symmetrical model, is a 3 cm long, 0.146 cm (17G) wide electrode or 2.5 cm cluster electrodes (Figure 1). Surrounding this is an inner compartment of 4 cm length of a variable diameter measuring 1–5 cm (simulating tumors of corresponding diameters). For two-compartment modeling, a range of varied inner (0–5 kg/m$^3$-s) and outer (0–5 kg/m$^3$-s) perfusions were used for each tumor size. The inner and outer electrical and thermal conductivities were varied as described above. The remainder of the underlying tissue characteristics were standardized and identical for both the inner and outer compartments and were selected to approximate normal liver parenchyma (including specific permittivity of 2000, specific heat of 3400 J/Kg-°C) [34].

*Outcome measurements*

The primary measurement used to evaluate RF heating patterns was the 50°C isotherm (i.e., the distance from RF electrode at which the temperature of the tissue is simulated to be 50°C at the end of the RF ablation session), as this has been used in the past to represent the standardized clinically relevant outcome (i.e., the temperature above which the tissue is completely irreversibly coagulated) for high-energy point-source tissue ablation [20]. For two-compartment models, the times required to achieve a minimum 50°C temperature at specified distances from the electrode, specifically at the tumor margin and an 'ablative margin' of normal tissue (defined as 5 mm of surrounding normal tissue beyond the tumor margin [35]) was also recorded (Figure 2).

*Data analysis*

For both single and cluster electrodes, resultant 50°C isotherms were used to construct contour maps (surface responses) expressing the relationship between inner and outer perfusion and heating, using Dataplot graphing software (D-plot, Vicksburg, MS). Separate surface responses were created for different tumor sizes (2–5 cm diameter) and single and cluster electrodes. Additionally, surface contour plots were also constructed demonstrated the 50°C isotherms for varying RF times (6–20 min) for both single and cluster electrodes.

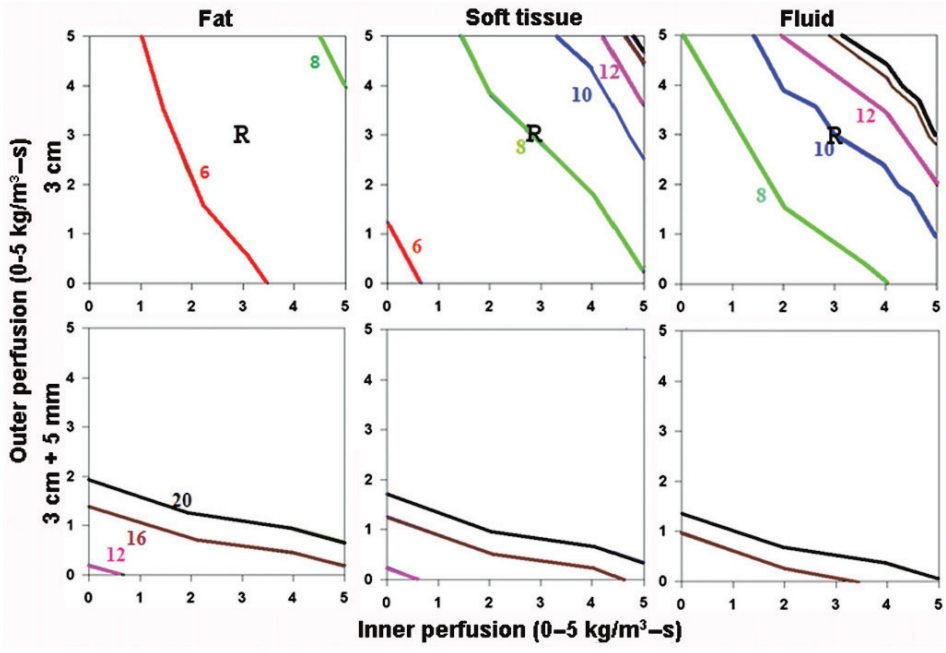


Figure 2. Effect of varying outer tissue thermal conductivity on RF heating for a 3 cm single electrode. This figure demonstrates the differences in the time required to achieve 50°C, using an internally cooled 3 cm single electrode, of the entire 3 cm tumor (0.5 W/m-°C) (without (top) and with (bottom) a 5 mm ablative margin) surrounded by fat (left, 0.23 W/m-°C), soft tissue (middle, 0.5 W/m-°C), and fluid (right, 0.7 W/m-°C), for varying inner tumor (*y*-axis) and outer tissue (*x*-axis) perfusions. Increasing the outer tissue thermal conductivity (fluid > soft tissue > fat) increases the time required to achieve ablation of the tumor alone from 6-8 min (fat) to up to 20 min (fluid), and at high perfusion states, complete ablation cannot be achieved. As an example, in treating renal cell carcinoma, with representative inner/outer perfusion characteristics (3 kg/m$^3$-s and 3 kg/m$^3$-s, respectively) denoted by the 'R', the outer thermal conductivity clearly influences the time required to achieve ablation.

For the purposes of this study, complete ablation could not be achieved if greater than 20 min was required (as denoted by the white area of the graph beyond the 20-min line in the figures, where applicable), as this is a commonly used clinical guideline.

## Results

### *Phase 1: Effect of varied thermal conductivity superimposed on a range of perfusions*

Increasing surrounding tissue thermal conductivity (i.e., from fat to soft tissue to fluid; 0.23–0.7 kg/m$^3$-s), increases the time required to achieve complete ablation such that tumor surrounded by fluid takes longer compared to soft tissue, followed by fat. This effect was most apparent at lower perfusions; as it was more difficult to achieve complete ablation at higher tumor/surrounding tissue perfusions regardless of surrounding tissue thermal conductivity (Figure 2). For example, inner thermal conductivity of soft tissue surrounded by fat had the greatest tumor heating in the shortest time, while ablation of soft tissue surrounded by ascites often could not be achieved despite increased heating times up to 20 minutes (Figure 2). As a clinical example, in treating renal cell carcinoma (with representative inner/outer perfusion characteristics denoted by the 'R' in Figure 2), increasing outer thermal conductivity increases the time required to achieve ablation.

Additionally, trying to achieve a 5 mm ablative margin around the tumor not only required longer ablation times but was more dependent on surrounding tissue perfusion, and was more difficult to achieve at higher perfusions. Also, there was a smaller difference between the times required to achieve complete ablation of the tumor with a 5 mm ablative margin for different surrounding thermal conductivities compared to tumor alone (Figure 2). These findings of RF heating patterns were similar for both a 3 cm single and 2.5 cm cluster electrode, though the 2.5 cm cluster electrode could achieve ablation in shorter RF times and for larger tumors, though again, this effect was most evident at lower perfusions. For example, the 2.5 cm cluster electrode could treat nearly all 3 cm tumors within 20 minutes, and a greater number of larger sized tumors (4–5 cm) (Figure 3), though this was limited to tumors/tissues

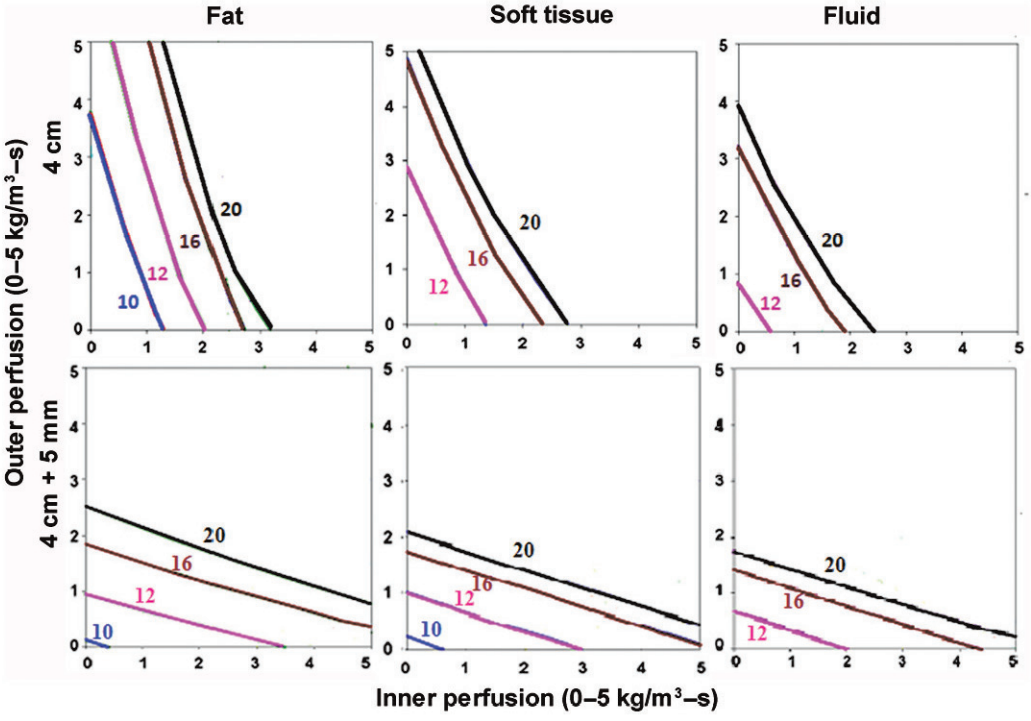


Figure 3. Effect of varying outer tissue thermal conductivity on RF heating for a 2.5 cm cluster electrode. This figure demonstrates the differences in the time required to achieve 50°C, using an internally cooled 2.5 cm cluster electrode, of the entire 4 cm tumor (0.5 W/m-°C) (without (top) and with (bottom) a 5 mm ablative margin) surrounded by fat (left, 0.23 W/m-°C), soft tissue (middle, 0.5 W/m-°C), and fluid (right, 0.7 W/m-°C), for varying inner tumor (*y*-axis) and outer tissue (*x*-axis) perfusions. Similar to findings in Figure 2 for a single electrode, perfusion demonstrates a dominant effect in all situations. Achieving an additional 5 mm ablative margin is also predominantly limited by high perfusions, though thermal conductivity does minimally effective ablation for surrounding fluid compared to fat/soft tissue. Inner perfusion has a dominant effect when trying to ablate the tumor alone, compared to including an ablative margin, where outer perfusion is more dominant. Increasing outer thermal tissue conductivity increases the time required for a given ablation, and can limit ablation success at higher perfusion states.

with lower perfusions (<4 kg/m$^3$-s inner and outer perfusions).

*Phase II: Effect of varied electrical conductivity superimposed on a range of perfusions*

For varied electrical conductivity, the greatest heating occurred for tumor surrounding by lung tissue (lowest; $\chi(I) = 0.5$, $\chi(O) = 0.1$ S/m), followed by tumor surrounded by soft tissue (intermediate, $\chi(I) = 0.5$, $\chi(O) = 0.5$ S/m), with the least heating seen for tumor surrounded by normal kidney (highest, $\chi(I) = 0.5$, $\chi(O) = 3.3$ S/m) (Figure 4). For example, attempting to achieve complete ablation plus a 5 mm ablative margin of background tissue required longer heating times and was more dependent on background tissue perfusion levels (and not possible at higher perfusions). The overall heating patterns were similar for all tumor sizes, though larger sized tumors required longer heating times. As a clinical example, in hepatocellular carcinoma (with representative inner/outer perfusion characteristics denoted by the 'H' in Figure 5), the outer thermal conductivity clearly influences the time required to achieve ablation, if this can be achieved at all. Furthermore, the heating patterns were similar for both the 3 cm single and 2.5 cm cluster electrode, though larger sized tumors could be treated by the cluster electrode.

Increasing the inner tumor electrical conductivity by simulated adjuvant saline injection ($\chi(I) = 0.5$ $\chi(O) = 0.5$ S/m) decreased RF times, and allowed complete ablation of cases with higher inner/outer perfusions compared to normal tumor (Figure 5).

*Phase III: Computer modeling of the 'best' and 'worst' clinical scenarios with varied thermal and electrical conductivity*

When assessing the 'best' (i.e., simulating saline injected around the electrode surrounded by soft tissue (electrical inner and outer conductivity of 4.0 and 0.5 S/m, respectively), surrounded by fat (thermal inner and outer conductivity of 0.5 and 0.23 W/m-°C, respectively)) and 'worst' clinical scenarios (i.e. simulating tumor in kidney (electrical inner and outer conductivity of 0.5 and 3.3 S/m, respectively), surrounded by ascites (thermal inner and outer conductivity of 0.5 and 0.7 W/m-°C, respectively)) for a 3 cm single electrode, the greatest

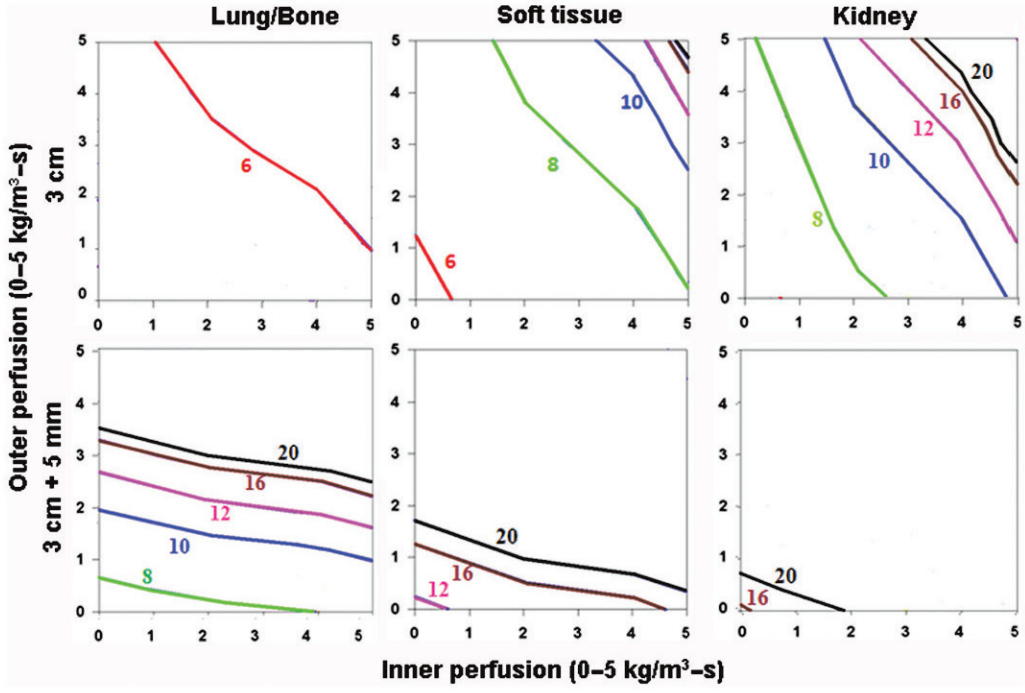


Figure 4. Effect of varying outer tissue electrical conductivity on RF heating for a 3 cm single electrode. This figure demonstrates the differences in the time required to achieve 50°C, using an internally cooled 3 cm single electrode, of the entire 3 cm tumor (0.5 S/m) (without (top) and with (bottom) a 5 mm ablative margin) surrounded by lung/bone (left, 0.1 S/m), soft tissue (middle, 0.5 S/m), and kidney (right, 3.3 S/m), for varying inner tumor ($y$-axis) and outer tissue ($x$-axis) perfusions. Increasing the outer tissue electrical conductivity (kidney > soft tissue > lung/bone) increases the time required to achieve ablation of the tumor alone from 6–8 min (lung/bone) to up to 20 min (kidney), and at certain high perfusion states, complete ablation cannot be achieved. Again, when trying to achieve an ablative margin, outer perfusion is more dominant, though in the absence of perfusion, outer thermal conductivity affects the time required to ablate the tumor.

effects of thermal and electrical conductivity were seen in the 3–4 cm tumor range (Figure 6), as almost all 2 cm, and almost no 5 cm tumors could be treated. For example, in the setting of saline injected around the electrode in a tumor surrounded by fat, the entire 3 cm tumor could be treated within 8–10 minutes, and almost the entire tumor with a 5 mm ablative margin could be treated within 20 minutes. Compared to this, a similarly sized renal tumor surrounded by ascites took longer to heat, and could not be completely treated at higher tissue and tumor perfusions (greater than 4 kg/m$^3$-s inner and outer perfusion). Additionally, a 5 mm ablative margin could not be achieved, except in the setting of almost no perfusion. For a 2.5 cm cluster electrode, almost all 2 and 3 cm tumors could be treated, regardless of the thermal and electrical conductivity characteristics. However, for larger tumors (4–5 cm), a similar pattern existed, where tumors with the 'best' tissue characteristics, both without (Figure 7) and with (Figure 8) a 5 mm ablative margin, could be treated in a shorter time, and at higher tumor and tissue perfusion states than the 'worst' combination of characteristics.

## Discussion

As RF ablation's therapeutic benefit is increasingly demonstrated in a wide range of tumor and tissue types, further characterization and understanding of the role of intrinsic tumor and tissue characteristics will be critical for optimizing RF energy delivery paradigms, and improving overall RF predictability. While prior modeling studies have studied the role of thermal and electrical conductivity in single and two compartment models [19–21, 29], those studies have been limited in that they evaluated the effects of electrical and thermal conductivity and perfusion individually and for a limited number of tissues, while in clinical reality, these characteristics vary in combination for many tumors and tissues [34]. Accordingly, this study combines modeling of these characteristics in clinically relevant settings of varied underlying tumor and surrounding tissue perfusion,

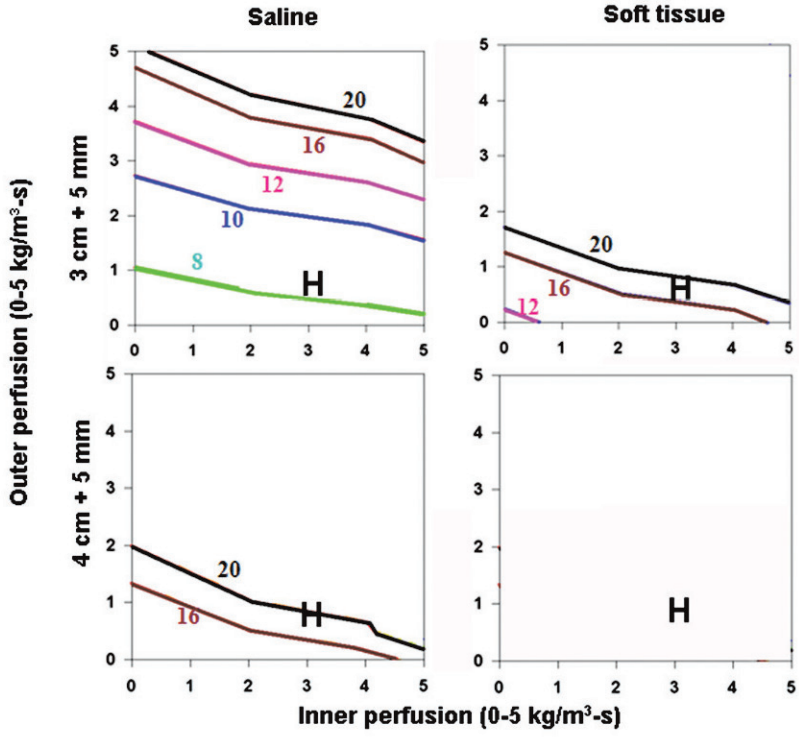


Figure 5. Effect of varying inner tissue electrical conductivity on RF heating for a 3 cm single electrode. This figure demonstrates the differences in the time required to achieve 50°C, using an internally cooled 3 cm single electrode, of both 3 (top) and 4 (bottom) cm tumors including a 5 mm ablative margin, infused with adjuvant saline (left, 4.0 S/m) or surrounded by soft tissue (right, 0.5 S/m), for varying inner tumor (*y*-axis) and outer tissue (*x*-axis) perfusions. Increasing the inner tissue electrical conductivity (adjuvant saline > soft tissue) decreases the time required to achieve ablation of the tumor alone from 12–20 min to up to 8 min, and increases the range of inner/outer perfusions at which tumors can be completely ablated. As an example, in hepatocellular carcinoma, with representative inner/outer perfusion characteristics (hypervascular HCC with an inner perfusion of 3.3 kg/m$^3$-s, surrounded by cirrhotic liver with an outer perfusion of 1 kg/m$^3$-s) denoted by the 'H', the outer thermal conductivity clearly influences the time required to achieve ablation, if this can be achieved at all.

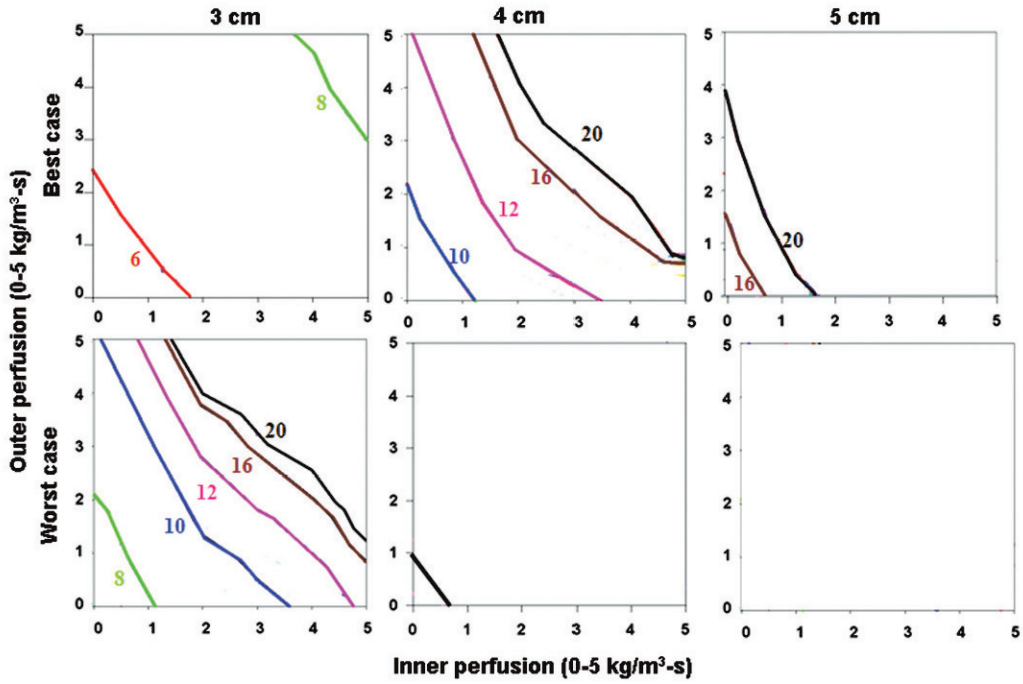


Figure 6. Comparing the effects of varying electrical and thermal conductivity for 'best' and 'worst' case scenarios for a 3 cm single electrode. This figure demonstrates the differences in the time required to achieve 50°C for varying inner tumor and outer tissue perfusions, using an internally cooled 3 cm single electrode for 3–5 cm tumors, with the 'best' (top, simulating adjuvant saline injecting in tumor (electrical inner and outer conductivity of 4.0 and 0.5 S/m, respectively), surrounded by fat (thermal inner and outer conductivity of 0.5 and 0.23 W/m-°C, respectively)) and 'worst' (bottom, simulating RCC in normal kidney (electrical inner and outer conductivity of 0.5 and 3.3 S/m, respectively), surrounded by ascites (thermal inner and outer conductivity of 0.5 and 0.7 W/m-°C, respectively)) scenarios based upon varying thermal and electrical conductivities. Significant differences can be seen between the 'best' and 'worst' combinations of electrical and thermal conductivity on the times required to achieve ablation and the range of tissue perfusions at which ablation can be achieved. For example, all 3 cm tumors regardless of perfusion can be ablated, compared to only those with lower inner/outer perfusion for 5 cm tumors. A similar pattern is seen when also trying to achieve an ablative margin.

to characterize the extent in which clinically relevant effects may occur.

The results of our study confirm prior work demonstrating that tissue perfusion remains the dominant tissue characteristic influencing RF heating, as has been well-documented in multiple prior experimental, clinical, and recent modeling studies [17, 21, 36]. However, continued variation in treatment outcomes and the ability to successfully treat tumors is also influenced by other tissue characteristics such as thermal and electrical conductivity. This effect is most apparent in the clinically relevant range of tumor sizes (3–5 cm) and treatment application times (8–20 minutes), and in commonly encountered clinical scenarios. For example, the presence of fat surrounding the tumor (with lower outer thermal conductivity) continues to increase inner tumor heating, and reduces the time required to achieve complete ablation. Interestingly, computer modeling of often-encountered clinical scenarios can provide insight into clinical observations already reported in the literature. For example, Gervais et al. document the difficulties in achieving complete tumor ablation in central renal tumors compared to exophytic renal tumors surrounded by perirenal fat [37]. Our results demonstrate that this effect is likely related to the lower thermal conductivity of fat, which serves as a heat insulator for tumor ablation. Indeed, insight into these effects may ultimately yield strategies to modify these characteristics in a manner that could improve overall RF ablation efficacy.

Our results further confirm the clinical relevance of surrounding tissue electrical conductivity, even in the presence of underlying tissue perfusion. Prior experimental and clinical studies have demonstrated the utility of modifying tissue electrical conductivity by injecting adjuvant saline around the electrode [16, 38, 39], findings which are reproduced in this modeling effort. Additionally, our results also suggest that underlying unfavorable tumor and surrounding tissue electrical conductivity characteristics of normal renal tissue around an RCC may contribute, along with the more well-known effect of high tissue perfusion, to the clinical difficulties in treating these tumors, including obtaining an ablative margin [40]. Furthermore, characterization of all

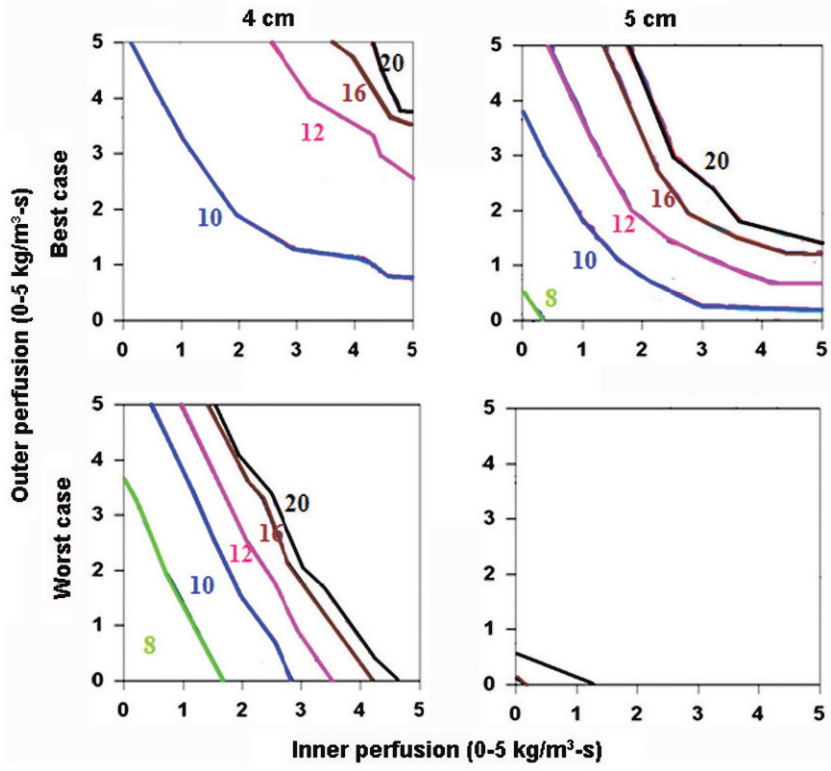


Figure 7. Comparing the effects of varying electrical and thermal conductivity for 'best' and 'worst' case scenarios for a 2.5 cm cluster electrode. This figure demonstrates the differences in the time required to achieve 50°C for varying inner tumor and outer tissue perfusions, using an internally cooled 2.5 cm cluster electrode for 4–5 cm tumors, with the 'best' (top, simulating adjuvant saline injecting in tumor (electrical inner and outer conductivity of 4.0 and 0.5 S/m, respectively), surrounded by fat (thermal inner and outer conductivity of 0.5 and 0.23 W/m-°C, respectively)) and 'worst' (bottom, simulating RCC in normal kidney (electrical inner and outer conductivity of 0.5 and 3.3 S/m, respectively), surrounded by ascites (thermal inner and outer conductivity of 0.5 and 0.7 W/m-°C, respectively)) scenarios based upon varying thermal and electrical conductivities. As for the single electrode, significant differences can be seen between the 'best' and 'worst' combinations of electrical and thermal conductivity on the times required to achieve ablation and the range of tissue perfusions at which ablation can be achieved.

three tissue characteristics simultaneously for commonly encountered clinical scenarios demonstrates that there are significant differences in tissue heating between those that have optimal tissue characteristics and those that do not. These findings are useful in that they identify those scenarios that will have the greatest potential for RF ablation success, and provide insight as to why RF ablation may be less successful in other scenarios.

Our study suggests that with further refinement and validation, computer modeling of tumor and surrounding tissue perfusion characteristics for specific tumors, may permit prediction of the likelihood of achieving complete ablation with currently recommended RF ablation strategies (i.e, 3 cm single or 2.5 cm cluster electrode for 12 minutes), and determine the optimal (either shorter or longer) times required to treat different tumors. Additionally, as clinical studies have demonstrated, achieving optimal tumor ablation includes ablating at least a 5 mm margin of surrounding normal-appearing background tissue [35], our results support recent studies that have demonstrated that differences in tumor/background characteristics can determine if and when ablation of a peripheral margin can be achieved [20, 29]. Given the well-documented difficulties in achieving complete RF ablation of larger tumors, especially in the liver, using differences in tumor/background characteristics in conjunction with tumor size may help to identify which tumors have a higher likelihood for success with RF treatment. Alternatively, in those tumors that are unlikely to be completely ablated with the existing clinical RF paradigms, further modeling may allow us to identify the extent of ablation that can be achieved with a single RF application, which can help design the more robust protocols for 'overlapping' ablations [41, 42].

Our results, along with prior studies, demonstrate that generation of surface response maps using data

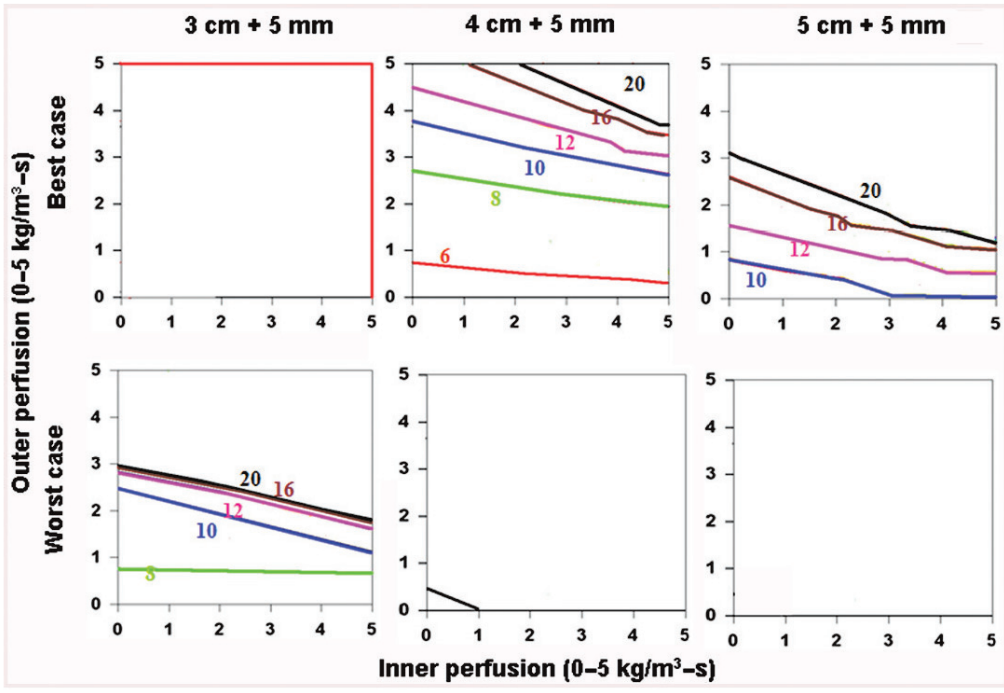


Figure 8. Comparing the effects of varying electrical and thermal conductivity for 'best' and 'worst' case scenarios. This figure demonstrates the differences in the time required to achieve 50°C for varying inner tumor and outer tissue perfusions, using an internally cooled 2.5 cm cluster electrode for 3–5 cm tumors with a 5 mm ablative margin, with the 'best' (top, simulating adjuvant saline injecting in tumor (electrical inner and outer conductivity of 4.0 and 0.5 S/m, respectively), surrounded by fat (thermal inner and outer conductivity of 0.5 and 0.23 W/m-°C, respectively)) and 'worst' (bottom, simulating RCC in normal kidney (electrical inner and outer conductivity of 0.5 and 3.3 S/m, respectively), surrounded by ascites (thermal inner and outer conductivity of 0.5 and 0.7 W/m-°C, respectively)) scenarios based upon varying thermal and electrical conductivities. Additionally, the ability to achieve ablation of a 5 mm margin is more dependent on outer perfusion (as demonstrated by the horizontally oriented isotherms) compared to achieving complete ablation without a margin (which is more dependent on inner perfusion, see Figure 7 for example).

from multiple simulations from computer modeling of the Bioheat equation continues to be a robust strategy for optimizing and evaluating RF ablation techniques [19–21, 23, 29, 36]. Specifically, the differing influences of tumor and surrounding tissue characteristics on RF heating patterns and the ability to achieve complete tumor ablation without and with a 5 mm ablative margin underscores the necessity of using a two-compartment model to accurately characterize RF tissue heating patterns. Indeed, in this paper we show how this mapping of trends in tissue heating can help explain why several RF tissue interactions can significantly influence both how required RF application time will vary, or if complete ablation is even achievable for varying clinical scenarios. Additionally, given that current clinical RF paradigms, and the most clinical experience, are based upon treatment of hepatic tumors, optimized RF ablation techniques in other tissues will likely require differing amounts of RF application time based upon differences in tissue characteristics.

While these initial results shed further insight into the role of RF tissue interactions on RF induced heating, there are several limitations of this study. Although several prior studies have used this model in characterization of the effects of both electrical and thermal conductivity on RF ablation with good *ex vivo* correlation [25, 29], further correlation of these findings to *in vivo* models will be required. Indeed, this study represents only one step forward towards the ultimate goal of developing clinically relevant predictive computer models based upon measured parameter inputs, and therefore, we caution against over-interpreting these results. Our modeling assumes that 50°C is an absolute thermal threshold for tissue destruction when, in fact, RF thermal dosimetry is likely to vary, as different tissues demonstrate varying tissue-specific thermal sensitivities [43]. Additionally, we assume tissue perfusion homogeneity and as yet have not incorporated the potential effect of larger vessels that are known to induce 'heat-sink' and influence ablation shape and outcome [17, 36, 44]. Thus, further refinements in defining endpoints may ultimately be needed for true predictability. Regardless, the current strategy of characterizing RF tissue interactions by isolating and

modulating individual parameters has already expanded our understanding of clinical RF ablation. Finally, to ultimately translate this into clinical practice, our approach assumes that the various tissue characteristics can be accurately measured in an *in vivo* setting. To this end, recent studies have examined the role of CT perfusion and MR arterial spin labeling to characterize tumor perfusion [45–48], and the development of micro-probes in assessing *in vivo* tissue electrical and thermal conductivities [49, 50], suggesting the potential for translating our findings into improvements in pre-procedure planning and better accuracy of RF ablation.

In conclusion, systematic two-compartment finite-element computer modeling of RF ablation demonstrates that while tissue perfusion has the dominant effect on RF heating, thermal and electrical conductivity are also important influences. Furthermore, optimal combinations of thermal and electrical conductivity can partially negate the effect of perfusion, and suboptimal thermal and electrical conductivity markedly limit successful ablation except in the setting of almost non-existent perfusion for clinically relevant tumor sizes. Knowledge of these are an important and necessary next step in rationally refining and tailoring optimal RF algorithms for specific clinical scenarios.

**Acknowledgements**

Supported by a grant from the National Cancer Institute, National Institutes of Health, Bethesda, MD (RO1-CA87992-01A1) and Valleylab, Boulder, Colorado, USA. Supported by the Tyco Healthcare/Mallinkrodt/RSNA Research Resident Grant from the RSNA Research & Education Foundation, Oak Brook, Illinois, USA (RR0603).

**Declaration of interest:** The authors report no conflicts of interest. The authors alone are responsible for the content and writing of the paper.

## References

1. Curley SA, Izzo F, Ellis LM, Nicolas Vauthey J, Vallone P. Radiofrequency ablation of hepatocellular cancer in 110 patients with cirrhosis. Ann Surg 2000;232:381–391.
2. Solbiati L, Livraghi T, Goldberg SN, Ierace T, DellaNoce M, Gazelle GS. Percutaneous radiofrequency ablation of hepatic metastases from colorectal cancer: Long term results in 117 patients. Radiology 2001;221:159–166.
3. Livraghi T, Meloni F, Morabito A, Vettori C. Multimodal image-guided tailored therapy of early and intermediate hepatocellular carcinoma: Long-term survival in the experience of a single radiologic referral center. Liver Transpl 2004;10:S98–106.
4. Livraghi T, Goldberg SN, Monti F, et al. Saline-enhanced radiofrequency tissue ablation in the treatment of liver metastases. Radiology 1997;202:205–210.
5. Lencioni R, Cioni D, Crocetti L, et al. Early-stage hepatocellular carcinoma in patients with cirrhosis: Long-term results of percutaneous image-guided radiofrequency ablation. Radiology 2005;234:961–967.
6. Gervais DA, McGovern FJ, Arellano RS, McDougal WS, Mueller PR. Renal cell carcinoma: Clinical experience and technical success with radio-frequency ablation of 42 tumors. Radiology 2003;226:417–424.
7. Dupuy DE, Mayo-Smith WW, Abbott GF, DiPetrillo T. Clinical applications of radio-frequency tumor ablation in the thorax. Radiographics 2002;22:S259–269.
8. Zagoria RJ, Chen MY, Kavanagh PV, Torti FM. Radio frequency ablation of lung metastases from renal cell carcinoma. J Urol 2001;166:1827–1828.
9. Dupuy DE, Hong R, Oliver B, Goldberg SN. Radiofrequency ablation of spinal tumors: Temperature distribution in the spinal canal. AJR Am J Roentgenol 2000;175:1263–1266.
10. Rosenthal DI, Hornicek FJ, Wolfe MW, Jennings LC, Gebhardt MC, Mankin HJ. Percutaneous radiofrequency coagulation of osteoid osteoma compared with operative treatment. J Bone Joint Surg Am 1998;80:815–821.
11. Goss SA, Johnston RL, Dunn F. Comprehensive compilation of empirical ultrasonic properties of mammalian tissues. 1978;64:423–457.
12. Gabriel S, Lau RW, Gabriel C. The dielectric properties of biological tissues: III. Parametric models for the dielectric spectrum of tissues. Phys Med Biol 1996;41:2271–2293.
13. Goldberg SN, Gazelle GS, Mueller PR. Thermal ablation therapy for focal malignancy: A unified approach to underlying principles, technqiues, and diagnostic imaging guidance. Am J Radiol 2000;174:323–331.
14. Pennes H. Analysis of tissue and arterial blood temperatures in the resting human forearm. J Applied Physiology 1948;1:93–122.
15. Goldberg SN. Radiofrequency tumor ablation: Principles and techniques. Eur J Ultrasound 2001;13:129–147.
16. Goldberg SN, Ahmed M, Gazelle GS, et al. Radiofrequency thermal ablation with adjuvant saline injection: Effect of electrical conductivity on tissue heating and coagulation. Radiology 2001;219:157–165.
17. Lu DS, Raman SS, Vodopich DJ, Wang M, Sayre J, Lassman C. Effect of vessel size on creation of hepatic radiofrequency lesions in pigs: Assessment of the 'heat sink' effect. AJR Am J Roentgenol 2002;178:47–51.
18. Livraghi T, Goldberg SN, Lazzaroni S, et al. Hepatocellular carcinoma: Radio-frequency ablation of medium and large lesions. Radiology 2000;214:761–768.
19. Liu Z, Lobo SM, Humphries S, et al. Radiofrequency tumor ablation: Insight into improved efficacy using computer modeling. AJR Am J Roentgenol 2005;184:1347–1352.
20. Liu Z, Ahmed M, Weinstein Y, Yi M, Mahajan RL, Goldberg SN. Characterization of the RF ablation-induced 'oven effect': The importance of background tissue thermal conductivity on tissue heating. Int J Hyperthermia 2006;22:327–342.
21. Liu Z, Ahmed M, Sabir A, Humphries S, Goldberg SN. Computer modeling of the effect of perfusion on heating patterns in radiofrequency tumor ablation. Int J Hyperthermia 2007;23:49–58.
22. Tungjitkusolmun S, Staelin ST, Haemmerich D, et al. Three-dimensional finite-element analyses for radio-frequency hepatic tumor ablation. IEEE Trans Biomed Eng 2002;49:3–9.
23. Haemmerich D, Tungjitkusolmun S, Staelin ST, Lee Jr FT, Mahvi DM, Webster JG. Finite-element analysis of hepatic multiple probe radio-frequency ablation. IEEE Trans Biomed Eng 2002;49:836–842.

24. Lobo SM, Liu ZJ, Yu NC, et al. RF tumour ablation: Computer simulation and mathematical modelling of the effects of electrical and thermal conductivity. Int J Hyperthermia 2005;21:199–213.
25. Lobo SM, Afzal KS, Ahmed M, Kruskal JB, Lenkinski RE, Goldberg SN. Radiofrequency ablation: Modeling the enhanced temperature response to adjuvant NaCl pretreatment. Radiology 2004;230:175–182.
26. Goldberg SN, Dupuy DE. Image-guided radiofrequency tumor ablation: Challenges and opportunities - Part I. JVIR 2001;12:1021–1032.
27. Humphries S, Platt RC, Ryan TR. ETherm finite element modeling of electrical heating and non-linear thermal transport in biological media. Proc Amer Soc Mech Eng High Temp 1997;355:131–134.
28. Humphries S. Field solutions on computers. Boca Raton, FL: CRC Press; 1997, Sections 11.3, 11.4, 12.2 and 12.3.
29. Solazzo SA, Liu Z, Lobo SM, et al. Radiofrequency ablation: Importance of background tissue electrical conductivity - An agar phantom and computer modeling study. Radiology 2005;236:495–502.
30. Goldberg SN, Gazelle GS, Halpern EF, Rittman WJ, Mueller PR, Rosenthal DI. Radiofrequency tissue ablation: Importance of local temperature along the electrode tip exposure in determining lesion shape and size. Acad Radiol 1996;3:212–218.
31. Dewhirst MW, Gross JF, Sim D, Arnold P, Boyer D. The effect of rate of heating or cooling prior to heating on tumor and normal tissue microcirculatory blood flow. Biorheology 1984;21:539–558.
32. Yi M, Podhajsky RJ, Mahajan RL. Investigation of temperature elevation and saline injection induced electrical conductivity change of hepatic tissue by using microprobe. SPIE (Proceedings paper) 2007;6440:64400N.
33. Livraghi T, Meloni F, Goldberg SN, Lazzaroni S, Solbiati L, Gazelle GS. Hepatocellular carcinoma: Radiofrequency ablation of medium and large lesions. Radiology 2000; 214:761–768.
34. Duck FA. Physical properties of tissue: A comprehensive reference book. Academic Press 1990; Harcourt Brace Jovanovich, London.
35. Goldberg SN, Charboneau JW, Dodd 3rd GD, et al. Image-guided tumor ablation: Proposal for standardization of terms and reporting criteria. Radiology 2003;228:335–345.
36. Haemmerich D, Wright AW, Mahvi DM, Lee Jr FT, Webster JG. Hepatic bipolar radiofrequency ablation creates coagulation zones close to blood vessels: A finite element study. Med Biol Eng Comput 2003;41:317–323.
37. Gervais DA, McGovern FJ, Arellano RS, McDougal WS, Mueller PR. Renal cell carcinoma: Clinical experience and technical success with radio-frequency ablation of 42 tumors. Radiology 2003;226:417–424.
38. Burdio F, Berjano EJ, Navarro A, et al. RF tumor ablation with internally cooled electrodes and saline infusion: What is the optimal location of the saline infusion? Biomed Eng Online 2007;6:30.
39. Burdio F, Navarro A, Berjano EJ, et al. Radiofrequency hepatic ablation with internally cooled electrodes and hybrid applicators with distant saline infusion using an in vivo porcine model. Eur J Surg Oncol 2007;16134:822–830.
40. Dodd GD, III , Frank MS, Aribandi M, Chopra S, Chintapalli KN. Radiofrequency thermal ablation: Computer analysis of the size of the thermal injury created by overlapping ablations. AJR Am J Roentgenol 2001;177:777–782.
41. Dodd III GD, Soulen MC, Kane RA, et al. Minimally invasive treatment of malignant hepatic tumors: At the threshold of a major breakthrough. Radiographics 2000;20:9–27.
42. Patriciu A, Awad M, Solomon SB, et al. Robotic assisted radio-frequency ablation of liver tumors – randomized patient study. Med Image Comput Comput Assist Interv Int Conf Med Image Comput Comput Assist Interv 2005; 8:526–533.
43. Mertyna P, Hines-Peralta A, Liu ZJ, Halpern E, Goldberg W, Goldberg SN. Radiofrequency ablation: Variability in heat sensitivity in tumors and tissues. J Vasc Interv Radiol 2007; 18:647–654.
44. Steinke K, Haghighi KS, Wulf S, Morris DL. Effect of vessel diameter on the creation of bovine lung radiofrequency lesions in vivo: Preliminary results. J Surg Res 2005;124:85–91.
45. Hakime A, Peddi H, Hines-Peralta A, et al. CT perfusion for the determination of pharmacologically mediated blood flow changes in an animal tumor model. Radiology 2007; 243:712–719.
46. Sabir A, Wilcox CJ, Atkins MB, Kruskal JB, Raptopoulos V, Goldberg SN. Multislice CT perfusion imaging enables early detection of therapeutic response to antiangiogenic therapy. Radiology 2006;241(Suppl.):213 (Proceedings from RSNA 2006).
47. Wang J, Zhang Y, Wolf RL, Roc AC, Alsop DC, Detre JA. Amplitude-modulated continuous arterial spin-labeling 3.0-T perfusion MR imaging with a single coil: Feasibility study. Radiology 2005;235:218–228.
48. De Bazelaire C, Rofsky NM, Duhamel G, Michaelson MD, George D, Alsop DC. Arterial spin labeling blood flow magnetic resonance imaging for the characterization of metastatic renal cell carcinoma (1). Acad Radiol 2005; 12:347–357.
49. Yi M, Panchawagh HV, Podhajsky RJ, Mahajan RL. Micromachined hot-wire thermal conductivity probe for biomedical applications. SPIE; (Proceedings paper) 2007; 6440:644000.
50. Yi M, Panchawagh HV, Mahajan RL, Liu Z, Goldberg SN. Micromachined electrical conductivity probe for RF ablation of tumors. Proceedings of IMECE 2005: ASME International Mechanical Engineering Congress & Exposition 2005.